

# Properties of zonal flow transport bifurcations driven by drift wave turbulence

A. Kammel, K. Hallatschek

*Max-Planck-Institute for Plasma Physics, 85748 Garching, Germany*

## Introduction

Previously unobserved transport bifurcations in self-consistent simulations have been examined in drift wave turbulence runs. These distinct transport states, associated with density corrugations, are linked with an asymmetry in the turbulence-fed zonal flows - the flows opposite to the electron diamagnetic drift direction being sharper and deeper than their counterparts. Both quantitative and qualitative arguments to explain this phenomenon are presented.

These bifurcations can potentially be of relevance to the problem of internal transport barriers since the characteristics of these barriers depend on the properties of the drift wave turbulence, especially in the high gradient tokamak edge. Another application might possibly be geostrophic modes - the analogon to drift waves in planetary turbulence.

## Equation system, units and numerical simulations

The Hasegawa-Wakatani equation system utilized describes a turbulent cold-ion sheared-slab resistive drift-wave system:

$$d_t n = \hat{\rho}_s^2 \cdot d_t \nabla_{\perp}^2 \phi \quad (1)$$

$$d_t \nabla_{\perp}^2 \phi = -\partial_{\parallel}^2 (\phi - n) \quad (2)$$

where  $d_t = \partial_t + (\vec{z} \times \nabla_{\perp} \phi \cdot \nabla_{\perp})$ ,  $\partial_{\parallel} = \partial_z - 2\pi x \partial_y$  and  $\nabla_{\perp}^2 = \partial^2 / \partial x^2 + \partial^2 / \partial y^2$  while  $L_z (= 2\pi q R)$  serves as the parallel length scale.

The only relevant (dimensionless) parameter in the Hasegawa-Wakatani equations is the ratio

$$\hat{\rho}_s = \rho_s / L_{\perp} \quad (3)$$

of the 'ion sound Larmor radius' (for cold ions)

$$\rho_s = m v_{th} / eB = m \sqrt{T_e} / eB m_i \quad (4)$$

to the orthogonal length scale (the scale of maximal drift wave growth where relaxation frequency and diamagnetic drift frequency are equal)

$$L_{\perp} = \left( \frac{\pi q R}{s} \right)^{2/3} \left( \frac{n_0 \eta_{\parallel} T_e}{2e \sqrt{m_i} L_n} \right)^{1/3} \frac{m_e}{m_i B} \quad (5)$$

with  $\eta_{\parallel}$  as the parallel resistivity and  $L_n = -n(dx/dn)$ .

Time is normalized to  $t_0 = L_{\perp} / v_{dia,e^-}$  where  $v_{dia,e^-} = \frac{T_e}{eBL_n}$ .

These equations have been implemented in the two-fluid Braginskii code NLET.

Typical run parameters - using the previously defined units - are  $n_x = n_y = 512$ ,  $n_z = 32$ ,  $L_x = L_y = 29.3L_\perp$ ,  $L_z = 6.3qR$ , grid step size  $\approx 7.7 \cdot 10^{-3}$ , time step  $\approx 9.5 \cdot 10^{-5}$  and run time  $\approx 2.5 \cdot 10^1$ . Extensive convergence as well as consistency scans have been performed as well as detailed parameter scans for  $\hat{\rho}_s$  and its constitutive parameters.

### Growth rate and dominant scales

Due to a lack of a feasible decomposition for the sheared, non-orthogonal, nearly collinear eigensystem, it is impossible to develop single eigenvectors on their own. Since there is thus no easy way to reproduce the development of the states via the sheared eigensystem, the linear properties of the flow states can best be characterised by the eigenvalue of the unsheared system.

In the spirit of this idea and due the absence of growing eigenmodes for all  $s \neq 0$ , the general growth rate for modes in the shearless, non-adiabatic case, as derived from eqns. (1) & (2), is used:

$$\gamma = \Im(\omega) \approx \frac{k_\parallel^2}{k_\perp^2} \frac{(1 + \hat{\rho}_s^2 k_\perp^2)}{\left[ (1 + \hat{\rho}_s^2 k_\perp^2)^2 \left( \frac{k_\parallel^2}{k_y k_\perp^2} \right) + 1 \right]} \quad \text{for } 4k_\perp^3 \ll k_\parallel^2 \quad (k_\perp \hat{\rho}_s \lesssim 1) \quad (6)$$

which can be approximated by

$$\gamma = \omega^*{}^2 / \omega_\parallel = k_\perp^2 / \left( k_\parallel^2 / (k_\perp^2) \right) = k_\perp^4 / k_\parallel^2$$

The growth rate is used to determine the mixing length anomalous heat diffusion coefficient  $D = \gamma / \vec{k}_\perp^2$ . The orthogonal wavenumber upon which the coefficient depends is determined by one of two scales between which there is a transition - coinciding with the zonal flow onset - at approx.  $\hat{\rho}_s \approx 0.12 - 0.20$ :

- relaxation scale  $L_\perp$  dominant for  $\hat{\rho}_s < 0.12$ :  $\hat{D} = \hat{\gamma} / \hat{k}_\perp^2 |_{k_\perp=L_\perp^{-1}} = \hat{\gamma} / \hat{k}_\perp^2 |_{k_\perp=1} \propto \hat{\rho}_s^0$
- diam. drift scale  $\rho_s$  dominant for  $\hat{\rho}_s > 0.2$ :  $D_\rho = \gamma_\rho / k_{\rho\perp}^2 |_{k_\perp=\rho_s^{-1}} = \gamma_\rho / k_{\rho\perp}^2 |_{k_{\text{units}}=\hat{\rho}_s^{-1}} \propto \hat{\rho}_s^{-2}$  (each in units of  $L_\perp$ )

$$\Rightarrow \frac{D_\rho}{\hat{D}} = \hat{\rho}_s^{-2} \text{ (analytically) as compared to } \frac{D_\rho}{\hat{D}} = \hat{\rho}_s^{-2 \pm 0.1} \text{ (numerically)}$$

$D/D_\rho$  is asymptotically constant for small  $\hat{\rho}_s$  and, vice versa,  $D/\hat{D}$  for large  $\hat{\rho}_s$ .

### Transport bifurcations

Our findings mark the first observation of transport bifurcations with two stable gradients in self-consistent drift wave turbulence simulations. These transport bifurcations are associated with density corrugations representing stationary transport states with high diffusivity and low gradients at the flows in electron diamagnetic drift direction and lowered diffusivity and higher gradients for the opposite flows.

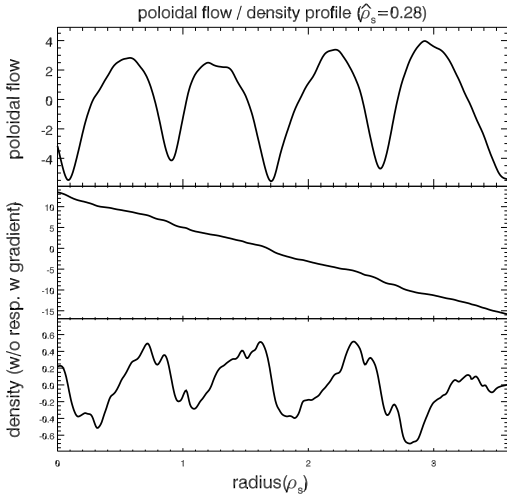


Figure 1: *Flow and density profiles*

### Bifurcation mechanism

Evaluating the drift wave action invariant  $N$  [2],

$$\partial_t N_{\vec{k}} = -\nabla_{\vec{x}} \left( N_{\vec{k}} \cdot \vec{v}_{gr, \vec{k}} \right) - \nabla_{\vec{k}} \left( N_{\vec{k}}(x) \cdot \vec{k}(\vec{x}, \vec{k}) \right) \quad (7)$$

positive flows - the ones in electron diamagnetic drift direction - are found to attract the turbulence while negative ones exhibit repulsive behavior. This can be understood more readily by inserting the shear-flow-dependent radial wavenumber

$$k_x = k_{x0} - \frac{\partial v_y}{\partial x} t |k_y| \quad \text{into} \quad v_{gr, x, cold} = \frac{\partial \omega}{\partial k_x} = \frac{-2k_x k_y \hat{\rho}_s^2}{[1 + \hat{\rho}_s^2 (k_x^2 + k_y^2)]^2} \quad (8)$$

$$\implies v_{gr, x} \approx -2k_{x0} k_y \hat{\rho}_s^2 + 2v_y' t k_y^2 \hat{\rho}_s^2 \quad \text{for} \quad (k_x^2 + k_y^2) \hat{\rho}_s^2 \ll 1 \quad (9)$$

The flows' shear changes the radial wavenumber of the propagating drift waves, acting like a forcefield. Flow shear as well as (due to  $v_{gr, x} \propto +v_y'$ ) the group velocity turn from positive to negative at the positive flows, leading to attraction and oscillation around those. Vice versa, the negative flows repulse the turbulence, making it impossible for modes with insufficient  $k_{x0}$  to penetrate them.

The drift waves originating at the negative flows are driven through an area of high flow shear equivalent to strongly increasing  $|k_x|$  and - due to the now non-negligible denominator - massively decreasing (or even halting) radial group velocity.

The flows exhibits a profound asymmetry (increasing for higher values of  $\hat{\rho}_s$ ) which accompanies the bifurcation, where the ones opposite to the electron diamagnetic drift direction are more sharply concentrated and more tightened radially.

This asymmetric flow pattern emerges on time scales of order  $\sim O(10^1)$  (taking approx. one order of magnitude longer for every doubling of  $\hat{\rho}_s$ ) for a typical parameter  $\hat{\rho}_s \approx 0.28$ . This long timescale, in combination with the high resolution, might indicate why these transport bifurcations seem to not have been observed in earlier studies[1].

This qualitative picture, supported by numerical studies, can help explain the simultaneous deepening of the negative flows and broadening of the positive flows through carry-off of positive- $k_y$  drift waves from the negative flows - even in the absence of density corrugations.

The same repulsion mechanism which is responsible for the flow asymmetry causes the density corrugations as well: Transport levels, in accordance with the repulsed turbulence, are reduced at the negative flows. But due to the perpetuation of the transport balance  $\partial_x \Gamma(x) = 0$  in the steady-state equilibrium, higher gradients at the negative flows are required to counterbalance the reduced turbulence levels - which leads to the observed density corrugations.

### Further studies

For analytical studies of the mechanism, an elementary nonlinear (to achieve a steady state) equation system with three balances from basic conservation principles has been proposed:

$$\mu[N] = v_y + \text{const.} \quad (\text{negative flows correlate with higher drift wave intensity}) \quad (10)$$

$$\Gamma[N] = \text{const.} \quad (\text{transport balance in equilibrium}) \quad (11)$$

$$\dot{N} = \gamma[v_y, n'] \quad (\text{change in drift wave intensity acc. to the local growth rate}) \quad (12)$$

Implementation of the resulting coupled equation system for drift wave intensity and flow strength yields asymmetric flows, in good agreement with the large-scale numerical simulations.

Another promising ansatz relies on the introduction of a nonlinear chemical potential  $\mu[N]$  (with  $\mu \propto N + N^2$  for large  $N$  and  $\mu \rightarrow -\infty$  for  $N \rightarrow 0$ ) and its three intersections with the drift wave momentum balance  $v = N + \text{const.}$ , yielding an unstable  $v_0$ -state as well as the two (stable) developed flow states. These have  $|v_+| \neq |v_-|$  because of to the intrinsic asymmetry in  $\mu[N]$ , causing an asymmetry of the radial flow length scale due to total flow conservation.

### Summary

Robust transport bifurcations in self-consistent drift wave turbulence simulations have been identified and examined in detail, including various parameter scans and an analysis of the dominant scales. The main features, the associated density corrugations and the flow asymmetry, have been explained qualitatively by transport and flow shear arguments, respectively. Further analytical mechanisms utilizing balances derived from basic conservation principles and the chemical potential serve to affirm the previous results.

### References

- [1] A. Zeiler, D. Biskamp, J.F. Drake and P.N. Guzdar, *Physics of Plasmas* **3**, 8, 2951-2960 (1996)
- [2] K. Itoh, K. Hallatschek, S.-I. Itoh, P.H. Diamond and S. Toda, *Physics of Plasmas* **12**, 062303 (2005)
- [3] K. Hallatschek and A. Zeiler, *Physics of Plasmas* **7**, 2554 (2000)